

Dispersion of Extremely Nondegenerate Nonlinear Refraction in Semiconductors

Peng Zhao¹, David J. Hagan¹ and Eric W. Van Stryland^{1,*}

¹CREOL, College of Optics and Photonics, University of Central Florida, Orlando, Florida 32816, USA

*Corresponding author: ewvs@creol.ucf.edu

Abstract—Dispersion of nondegenerate nonlinear refraction in semiconductors is measured using the Beam-Deflection technique. With large nondegeneracy, n_2 is greatly enhanced and exhibits a strong nonlinear dispersion, which rapidly switches sign to negative near the bandgap. Potential applications including nondegenerate all-optical switching and pulse shaping are discussed.

I. INTRODUCTION

In semiconductors, the bound-electronic nonlinear refraction (NLR) governs the refractive nonlinearity below the bandgap, of which the nondegenerate (ND) NLR, namely the refractive index change at frequency ω_a due to the presence of a beam at frequency ω_b , of coefficient $n_2(\omega_a; \omega_b)$, is much less explored compared to the degenerate case. This is particularly true for the extremely nondegenerate case (i.e. $\hbar\omega_a \gg \hbar\omega_b$) where two-photon absorption (2PA) is present [1]. Knowledge of the ND-NLR dispersion enables tailoring of a material's nonlinearities, allowing predictions of the best operating wavelengths of semiconductor photonic devices such as all-optical switches (AOS) [2].

Previously, we developed the theory to predict the NLR dispersion from a Kramers-Kronig transformation of its associated nondegenerate nonlinear absorption (ND-NLA) spectrum [3, 4]. The NLA arises from two-photon 2PA, electronic Raman and optical Stark effects [5]. With highly nondegenerate photon pairs, the two-photon transition rate is greatly enhanced because of the resonant enhancement of the small photon energy with the intraband self-transition and the larger photon energy with the interband transition [6-8]. Linked by the KK relations, this enhancement in ND-2PA translates to enhancement of ND-NLR. The theory predicts a positively enhanced n_2 near the resonance of the ND-2PA. This enhancement becomes larger with an increase in the nondegeneracy. In the extremely nondegenerate case, a strong anomalous nonlinear dispersion occurs near the bandgap, making the greatly enhanced n_2 rapidly switch sign to a large negative NLR over a very narrow spectral range.

II. EXPERIMENTS AND DISCUSSIONS

To experimentally investigate the dispersion of ND-NLR, we measured three direct-gap semiconductors (ZnO, ZnSe and CdS) using our recently developed Beam-Deflection (BD) technique [9]. BD is a highly sensitive excite-probe technique, where the strong excitation pulse at ω_b creates an index change via NLR that follows its spatial irradiance distribution, i.e.

Gaussian. The probe pulse at ω_a is focused to a smaller size and spatially displaced off the excitation beam's center. The index gradient deflects the probe which is measured with a position sensitive segmented detector by taking the difference of the energy falling on the left and right halves, $\Delta E = E_{left} - E_{right}$, and normalizing to the total energy E . The BD signal, $\Delta E/E$, is directly proportional to $n_2(\omega_a; \omega_b)$, and the transmission change in E is proportional to the NLA (i.e. 2PA). Here, the excitation wavelength is fixed at $\lambda_b = 2.3 \mu\text{m}$, and the probe is derived from a white-light continuum with wavelength selected at $\lambda_a = 430\text{-}750 \text{ nm}$ using bandpass interference filters.

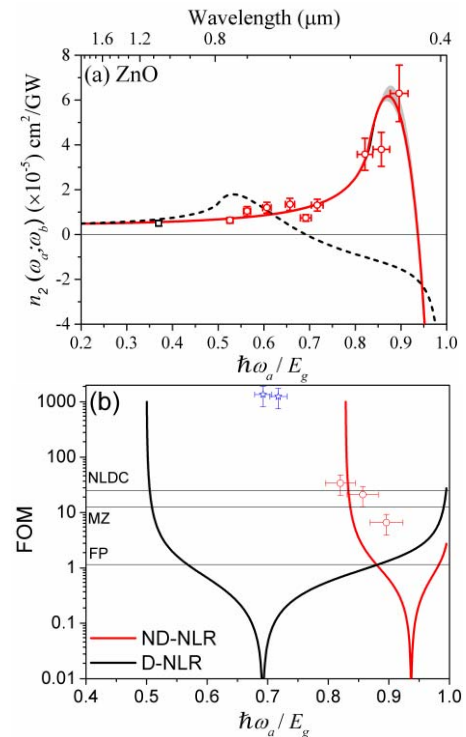


Figure 1. (a). Measured $n_2(\omega_a; \omega_b)$ dispersion (red) of ZnO, compared to theoretical calculations for nondegenerate (solid lines) and degenerate (dashed lines) n_2 ; degenerate n_2 data (black) is from [5]; (b). measured FOM of ND-NLR for ZnO in the presence of ND-2PA (red) and ND-3PA with $I_{sw} = 1 \text{ GW/cm}^2$ (blue), as compared to theory (solid lines). The minimum requirements for AOS geometries of a Mach-Zehnder (MZ) interferometer, nonlinear directional coupler (NLDC) and Fabry-Perot (FP) filter are shown for comparisons.

The measured ND-NLR dispersion of ZnO is shown in Figure 1 (a), where $\hbar\omega_b$ is $\sim 16\%$ of the bandgap. We measured values of n_2 close to the zero-frequency limit for $\hbar\omega_a/E_g <$

0.68, as no NLA occurs. For $\hbar\omega_a/E_g = 0.69$ and 0.72 , ND-3PA are measured along with ND-NLR. Due to the nondegenerate enhancement, significantly larger n_2 is measured for $\hbar\omega_a/E_g = 0.82 - 0.90$, where at $\lambda_a = 440$ nm, we measured an $n_2 \sim 12\times$ larger than the zero-frequency limit [5] and $\sim 3\times$ larger than the maximum of the calculated degenerate n_2 . But it should be noted that at the wavelength where n_2 reaches its maximum enhancement, ND-2PA is also greatly enhanced. The measured ND-NLR dispersion closely follows our earlier predictions [1].

The enhancement of NLR suggests advantages of the nondegenerate operating scheme of Kerr-effect based photonic devices such as AOS, where the signal beam, with $\hbar\omega_a$ close to the bandgap, can be modulated with an infrared control beam at $\hbar\omega_b$. A larger $n_2(\omega_a; \omega_b)$ results in a smaller switching irradiance, i.e. I_{sw} . A figure of merit (FOM) is defined as $4\pi|n_2/(\lambda_a\alpha_2)|$ and $8\pi|n_2/(3\lambda_a\alpha_3I_{sw})|$ respectively for 2PA or 3PA spectral regions [2]. The measured nondegenerate FOM of ZnO is shown in Figure 1 (b), as compared to the theory. The degenerate FOM is too small within its 2PA region, which essentially limits the operating wavelength to below half of the bandgap for all given AOS geometries. The ND-NLR scheme removes this limitation, as it shifts the 2PA resonance, and, in principle, allows any signal wavelength below the bandgap to be used without the presence of 2PA. With $I_{sw} = 1$ GW/cm², a FOM > 1000 is measured with ND-3PA as the dominant loss mechanism. Note the most enhanced n_2 , i.e. at $\lambda_a = 440$ nm, does not result in the largest FOM. This is because 2PA is also enhanced in this spectral region [7].

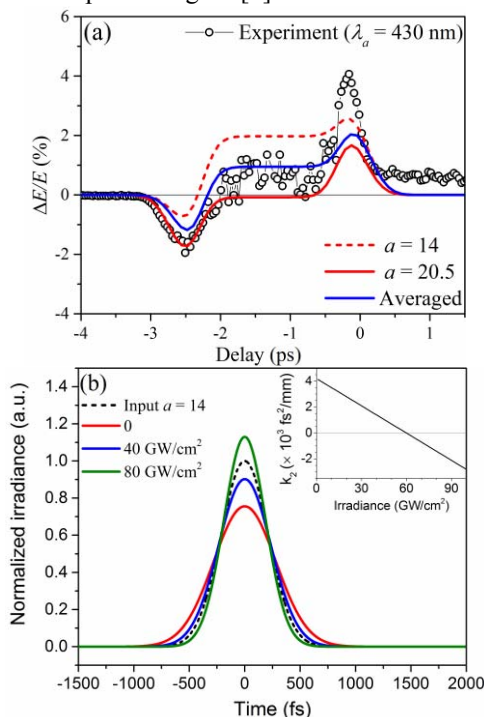


Figure 2. (a). Measured $\Delta E/E$ (black circles) of ZnO with probe at 430 nm, compared to theoretical predictions using chirping conditions at front (red dashed) and back (red solid) surface of the sample, along with the averaged curve (blue solid); (b) predictions of nonlinear pulse shaping effect at $\lambda_a = 430$ nm from the strong anomalous nonlinear dispersion of ND-NLR in ZnO.

By probing ZnO at $\lambda_a = 430$ nm with a 10 nm (FWHM) bandwidth, we cover the zero-crossing frequency of the strong anomalous dispersion range of ND-NLR. The higher and lower frequency components of the probe pulse will see a negative and positive n_2 , respectively. Due to the mismatch in group velocity, the excitation temporally overlaps the rising edge of the probe (lower frequency) at the front surface of the sample at zero delay, resulting in a positive signal, as shown in Figure 2 (a). The excitation pulse overlaps with the falling edge of the probe (higher frequency) at the back surface, giving a negative signal around ~ -2.5 ps delay. The experimental results show agreement with theoretical predictions considering a linearly up-chirped probe pulse with an instantaneous frequency $\omega_a = 2at/\tau_G^2$, where τ_G is the pulsewidth of the probe field ($\text{HW}^{1/e}$), a is the chirping parameter which is 14 for the initial input pulse and 20.5 after propagating through the sample due to the group velocity dispersion (GVD) of 4158 fs²/mm in ZnO.

The strongly dispersive ND-NLR significantly alters the material's dispersion, capable of providing a large and ultrafast spectral phase modulation on a femtosecond pulse with bandwidth centered near the zero-crossing frequency. As predicted in the inset of Figure 2 (b), due to the anomalous dispersion of ND-NLR ~ 430 nm in ZnO, the GVD factor k_2 decreases from its intrinsic value with an increase of the excitation irradiance. Above 60 GW/cm², k_2 becomes negative. This suggests potential applications for all-optical pulse shaping using the extremely ND-NLR in semiconductors.

This effect is predicted in Figure 2 (b) using theoretical ND-NLR dispersion. For the same incoming up-chirped probe pulse, the pulsewidth is broadened from 500 fs to 562 fs after propagating through the 0.5 mm thick ZnO sample as a result of the intrinsic GVD. With 40 GW/cm² excitation, this broadening is reduced to 532 fs. The pulse is compressed to 443 fs with a higher excitation irradiance of 80 GW/cm², however, the transmission is only $\sim 20\%$ due to ND-2PA. Another strong nonlinear dispersion occurs near the onset of 2PA, i.e. $\lambda_a = 473$ nm, where ND-NLR exhibits normal dispersion. This results in an increase of k_2 to 6800 fs²/mm under 60 GW/cm² excitation. The experimental demonstration of nonlinear pulse shaping is the subject of future work.

REFERENCES

1. M. Sheik-Bahae, J. Wang, and E. W. V. Stryland, *IEEE Journal of Quantum Electronics* **30**, 249-255 (1994).
2. P. Zhao, M. Reichert, D. J. Hagan, and E. W. Van Stryland, *Opt. Express* **24**, 24907-24920 (2016).
3. D. C. Hutchings, M. Sheik-Bahae, D. J. Hagan, and E. W. Stryland, *Optical and Quantum Electronics* **24**, 1-30 (1992).
4. M. Sheik-Bahae, in *Nonlinear Optical Materials*, J. V. Moloney, ed. (Springer New York, New York, NY, 1998), pp. 205-224.
5. M. Sheik-Bahae, D. C. Hutchings, D. J. Hagan, and E. W. Van Stryland, *Quantum Electronics*, *IEEE Journal of* **27**, 1296-1309 (1991).
6. J. A. Bolger, A. K. Kar, B. S. Wherrett, R. DeSalvo, D. C. Hutchings, and D. J. Hagan, *Optics Communications* **97**, 203-209 (1993).
7. C. M. Cirloganu, L. A. Padilha, D. A. Fishman, S. Webster, D. J. Hagan, and E. W. Van Stryland, *Opt. Express* **19**, 22951-22960 (2011).
8. D. C. Hutchings and E. W. Van Stryland, *J. Opt. Soc. Am. B* **9**, 2065-2074 (1992).
9. M. R. Ferdinandus, H. Hu, M. Reichert, D. J. Hagan, and E. W. Van Stryland, *Opt. Lett.* **38**, 3518-3521 (2013).